Research paper

Permeability prediction in tight carbonate rocks using capillary pressure measurements

F. Rashid[*], P.W.J. Glover, P. Lorinczi, D. Hussein, R. Collier, J. Lawrence

School of Earth and Environment, University of Leeds, UK

A B S T R A C T

The prediction of permeability in tight carbonate reservoirs presents ever more of a challenge in the hydrocarbon industry today. It is the aim of this paper to ascertain which models have the capacity to predict permeability reliably in tight carbonates, and to develop a new one, if required. This paper presents (i) the results of laboratory Klinkenberg-corrected pulse decay measurements of carbonates with permeabilities in the range 65 nD to 0.7 mD, (ii) use of the data to assess the performance of 16 permeability prediction models, (iii) the development of an improved prediction model for tight carbonate rocks, and (iv) its validation using an independent data set. Initial measurements including porosity, permeability and mercury injection capillary pressure measurements (MICP) were carried out on a suite of samples of Kometan limestone from the Kurdistan region of Iraq. The prediction performance of sixteen different percolation-type and Poiseuille-type permeability prediction models were analysed with the measured data. Analysis of the eight best models is included in this paper and the analysis of the remainder is provided in supplementary material. Some of the models were developed especially for tight gas sands, while many were not. Critically, none were developed for tight gas carbonates. Predictably then, the best prediction was obtained from the generic model and the RGPZ models ($R^2 = 0.923$, 0.920 and 0.915, respectively), with other models performing extremely badly. In an attempt to provide a better model for use with tight carbonates, we have developed a new model based on the RGPZ theoretical model by adding an empirical scaling parameter to account for the relationship between grain size and pore throat size in carbonates. The generic model, the new RGPZ Carbonate model and the two original RGPZ models have been tested against independent data from a suite of 42 samples of tight Solnhofen carbonates. All four models performed very creditably with the generic and the new RGPZ Carbonate models performing well ($R^2 = 0.840$ and 0.799, respectively). It is clear from this study that the blind application of conventional permeability prediction techniques to carbonates, and particularly to tight carbonates, will lead to gross errors and that the development of new methods that are specific to tight carbonates is unavoidable.

© 2015 Elsevier Ltd. All rights reserved.

1. Introduction

Fluid permeability (Bernabé and Maineult, 2015) is one of the most important parameters in reservoir characterisation and management. While measurable on core samples in the laboratory, permeability is not available directly from downhole measurements. Since core sample measurement is expensive and core samples only cover a small proportion of any reservoir interval, other methods are required. Consequently, there exists a plethora of empirical models which have been designed to calculate permeability from a wide range of proxy measurements that often can be made downhole. We can classify these models into different types.

One common type relates the absolute permeability to the grain size, pore size or pore-throat size of the rock. These models can be considered to be percolation or characteristic length scale models and relate the progress of the fluid through a porous medium, which can be described by flow through an aperture with a single length scale. Examples of this include the Kozeny-Carman (*e.g.*, Bernabé and Maineult, 2015; Schwartz et al., 1989), Katz and Thompson (Katz and Thompson, 1986, 1987; Thompson et al., 1987) and RGPZ (Glover et al., 2006a,b,c) models. Walker

* Corresponding author. Tel.: +44 7445291315.
 E-mail address: eefnr@leeds.ac.uk (F. Rashid).

and Glover (2010) considered the theoretical basis for all of these models.

A second common model treats flow paths in the rock as a bundle of tubes, each of which may have a different diameter. This is clearly a simplification of a porous medium, but it is a different simplification than that used by the characteristic length scale models. Some of these models include scaling coefficients, which enable this type of model to incorporate different connectivities. Such an approach is then beginning to converge with the electrical models represented by Archie's law (Archie, 1942), the modified Archie's law (Glover et al., 2000), and the generalised Archie's law for *n*-phases (Glover, 2010). Examples of this approach to permeability modelling include models by Swanson (1981), Wells and Amaefule (1985), Winland (Kolodzie, 1980), Huet et al. (2005), Pittman (1992), Kamath (1992) and Dastidar et al. (2007).

The main difference between the characteristic length scale (percolation) models and the Poiseuille-type models is that the latter defines and calculates the flow paths in the model exactly (as tubes) while the percolation models do not. Clearly, real rocks are rather more variable than the Poisseuille-type models assume, and that variability is built into the Poiseuille-type models by using empirical parameters that calibrate the model to a given formation in a given reservoir. Consequently, each calibrated prediction model is specific to a given reservoir, and errors would occur if the models were applied to another reservoir. This introduces an important restriction to the Poiseuille-type models which reduces their generality. However, in conventional reservoirs, the restriction is often balanced by the advantage that the quality of prediction in a well-calibrated formation of a particular reservoir is often extremely good.

By contrast, the characteristic length scale models build the variability of the porous medium into the model, describing flow through the medium in terms of a characteristic length scale. Often these length scales have a single value, such as the modal pore diameter in a pore size distribution of the rock. This can work well if the rock has a well-defined and narrow unimodal pore diameter distribution, but works less well if the rock has a wide or multi-modal pore diameter distribution. Sometimes such models are implemented using a distribution of characteristic length scales. The RGPZ model (Glover et al., 2006a,b,c), for example, has been implemented in such a way that the overall permeability of a rock was calculated from the geometric mean of the modal grain sizes weighted to account for the distribution of those grain sizes within the rock (Glover et al., 2006a,b,c). Such an approach makes the often unjustified assumption that the whole range of grain (pore or pore throat) sizes that are being averaged contribute to the permeability of the sample.

In this work almost all the models were developed initially for conventional reservoirs with permeabilities greater than 1 mD (Comisky et al., 2007), although a few more recent models, notably the Wells and Amaefule (1985) modification to the Swanson (1981) model and the Huet et al. (2005) model were created specifically for tight gas sands with micro-darcy permeabilities. None of the models tested in this paper have been developed for tight gas carbonates with permeabilities in the nano-darcy to micro-darcy range. As far as we are aware no models currently exist.

2. Permeability models

The experimental data obtained in this study have been used to evaluate 16 permeability models, which are listed in Table 1. In this table a distinction is made between empirical constants, which are constants that have been obtained empirically but are not usually allowed to vary in the application of the model, and fitting parameters, which are parameters that are commonly expected to be

varied in the application the model in order to make the model fit the data.

Eight of the sixteen models which were tested performed very badly when predicting the permeability of tight carbonate rocks. The description of these models and a full analysis of how well they performed has been excluded from this paper, but included as a file of Supplementary Material which can be downloaded from the publisher's website. The eight models which are included in the Supplementary Material encompass the Katz-Thompson models using critical lengths and electrical length models (Katz and Thompson, 1986, 1987; Thompson et al., 1987), the Swanson model (Swanson, 1981), the Wells-Amaefule model (Wells and Amaefule, 1985), the Kamath model (Kamath, 1992), the Huet et al. model (Huet et al., 2005), and the Berg Fontainebleau model (Berg, 2014). Three of these models are of the percolation-type, and the remaining five are of the Poiseuille-type.

All of the models listed in Table 1 can be implemented using data obtained from MICP measurements. The fundamental underlying equation which governs the MICP method is what we now call the Washburn equation (Washburn, 1921), which relates the capillary pressure P_c in a capillary tube of radius R, containing air and mercury in terms of the interfacial tension σ and the wetting angle θ.

$$P_c = \frac{2\sigma cos\theta}{R} \tag{1}$$

The Washburn equation should properly be called the Bell-Cameron-Lucas-Washburn equation because similar theoretical developments had been made three years before by Lucas (1918) upon work on capillary pressures by Bell and Cameron in 1906 (Bell and Cameron, 1906). For mercury and air, the interfacial tension $\sigma_{Hg-air} = 0.48$ N/m (480 dyn/cm) and the contact angle $\theta_{Hg-air} = 0°$. In SI units, the use of R in metres gives the capillary pressure in pascals. If imperial units are used, R in μm gives the capillary pressure in psi.

Permeability is similar to electrical conductivity in that it can be thought of as being partially controlled by the amount of pore space for hydraulic or fluid flow, and partially controlled by how connected that pore space is (*e.g.*, Glover, 2015). The assumption that underlies all of the permeability models is that there is a particular length scale, or distribution of length scales, that controls the permeability of the rock. In the case of the percolation models, that length scale is given explicitly in the model either as a characteristic length scale with an undefined physical expression, as the mean, modal or median grain diameter, as the pore diameter calculated with the theta transformation (Glover and Walker, 2009), or as some measure of the pore throat size such as that obtained from MICP measurements.

In the case of the Poiseuille models, the capillary pressure that corresponds to a given characteristic length through Eq. (1) is used. One must, therefore, chose which point on the capillary pressure curve to use in order to define the capillary pressure for permeability modelling. It is this capillary pressure will be associated with a particular wetting fluid saturation (air saturation for MICP measurements, and usually water saturation in the reservoir).

The most commonly used points on the capillary pressure curve are the entry pressure and threshold pressure (Fig. 1). The entry pressure on the mercury–injection curve is the point on the curve at which mercury initially enters the sample. This point is often indicative of the largest pore throat size present in the sample and is usually associated with the largest pores (Robinson, 1966). There is some uncertainty that such a measure really does represent the largest pore throat size because (i) we are limited to the sample size and larger samples may contain larger pore throats, and (ii)

Table 1
Fundamental properties and inputs of the sixteen models evaluated in this study.

Name	Parameters	No. of empirical constants	No. of fitting parameters	Reference
Percolation-based models				
Katz and Thompson – critical length	• Critical length, L_c • Formation factor	1	None	Katz and Thompson (1986, 1987), Thompson et al. (1987)
Katz and Thompson - maximum electrical conductance length	• Maximum electrical conductance length, L_{Emax} • Critical length, L_c • Fraction of Hg-filled pore volume at L_{Emax}, S_{LEmax} • Porosity, ϕ	1	None	Katz and Thompson (1986, 1987), Thompson et al. (1987)
Katz and Thompson - maximum hydraulic length	• Maximum hydraulic length, L_{Hmax} • Critical length, L_c • Fraction of Hg-filled pore volume at L_{Hmax}, S_{LEmax} • Porosity, ϕ	1	None	Katz and Thompson (1986, 1987), Thompson et al. (1987)
RGPZ theoretical approximate	• Characteristic grain diameter, d_{grain} • Cementation exponent, m • 'a'-parameter • Porosity, ϕ	1	None	Glover et al. (2006a,b,c)
RGPZ theoretical exact	• Characteristic grain diameter, d_{grain} • Cementation exponent, m • 'a'-parameter • Formation factor F, or porosity ϕ	1	None	Glover et al. (2006a,b,c)
RGPZ empirical carbonate	• Characteristic grain diameter, d_{grain} • Cementation exponent, m • 'a'-parameter • Formation factor F, or porosity ϕ	1	1	This work
Schwartz, Sen and Johnson (SSJ) generic form	• Characteristic pore size, Λ • Formation factor F	1	1	Johnson et al. (1986); Johnson and Schwartz (1989); Johnson and Sen (1988); Schwartz et al. (1989)
Berg (fontainebleau implementation)	• Porosity, ϕ	4	4	Berg (2014) Equation (53)
Berg generic model	• Effective porosity, ϕ_s • Effective hydraulic tortuosity, τ_s • Constriction factor, C_s • Characteristic length L_h (equal to the radius of a capillary tube)	1	None	Berg (2014) Equation (32)
Poiseuille-based models				
Swanson	• Apex value of Hg saturation to capillary pressure	2	2	Swanson (1981)
Wells-Amaefule	• Apex value of Hg saturation to capillary pressure	2	2	Wells and Amaefule (1985)
Kamath 'model'	• Apex value of Hg saturation to capillary pressure	2	2	Kamath (1992)
Winland	• Length at which a mercury saturation is 35%, R_{35} • Porosity, ϕ	3	3	Gunter et al. (2014)
Pittman	• Radius associated with the critical length L_c, R_{apex} • Porosity, ϕ	3	3	Kolodzie (1980)
Dastidar et al.	• Weighted geometric mean of the pore size, R_{wgm} • Porosity, ϕ	3	3	Dastidar et al. (2007)
Huet et al.	• Displacement pressure, P_d • Irreducible water saturation, S_{wi} • Porosity, ϕ • Brooks-Corey parameter, λ	5	5	Huet et al. (2005)

irregularities on the surface of the samples can mimic large pores and give erroneous results when Eq. (1) is applied to them. Consequently, the low-mercury saturation portion of the MICP curve may not be truly representative of the rock (Bliefnick and Kaldi, 1996).

The threshold pressure is that at which the saturation of mercury increases dramatically and corresponds graphically to an upward convex inflection point on the mercury–injection curve. It represents the capillary pressure at which the greatest population of pore sizes fill and for a unimodal pore throat size distribution indicates the pressure at which the mercury can for the first time access the pores which represent the main fraction of porosity in the rock. This point has been used profitably by Dewhurst et al. (2002) to quantify the capability of mud-rocks to trap high pressure fluids. The threshold pressure point has been experimentally determined by recording electrical resistance across a sample and measuring the pressures at which continuity occurs (Katz and Thompson, 1986, 1987; Thompson et al., 1987).

Pittman (1992) and Winland (Kolodzie, 1980; Comisky et al., 2007; Gunter et al., 2014) identified a mercury saturation percentile at which the reservoir threshold pressure can be predicted to occur. Values of 3%, 5% and 10% (Schowalter, 1979) of the total mercury saturation are considered by various researchers to predict the threshold pressure, although such artificial restrictions are of no real utility since the threshold pressure depends upon the rate of decrease of the tail of the pore throat size distribution which is sample-dependent.

2.1. Percolation-based models

2.1.1. Katz-Thompson [KT] models (Maximum Hydraulic Length)

The Katz and Thompson models (Katz and Thompson, 1986, 1987; Thompson et al., 1987) are based on percolation theory, and consider flow through a porous medium with random microstructure and connectivity. Flow is considered to be controlled by a length scale. There are three different length scales which are commonly used, each of which leads to a different permeability prediction model; the Critical Length (L_c), Maximum Hydraulic Length (L_{Hmax}) and Maximum Electrical Conductance Length (L_{Emax}). The Maximum Hydraulic Length (L_{Hmax}) is described here,
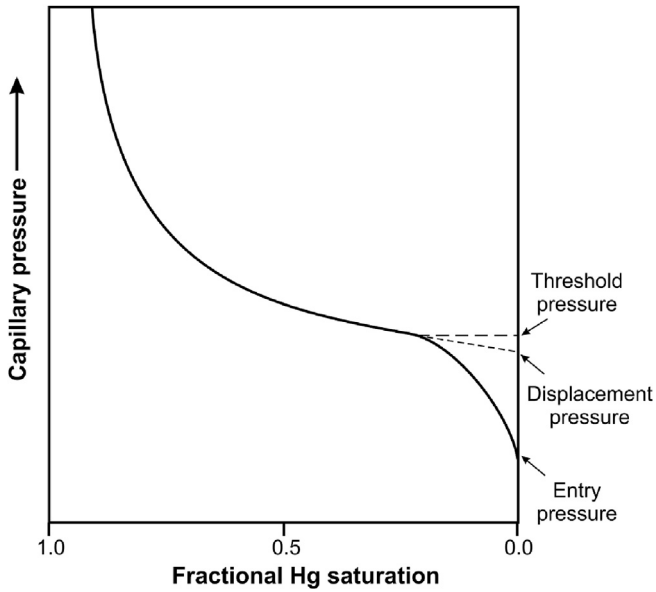
Fig. 1. Definition of the entry pressure, displacement pressure and threshold pressure of a MICP capillary pressure curve.

Fig. 2. A typical capillary pressure curve for the MICP technique imposed upon which the length scales from the various models are used in this work.

while the remaining two models are describe in the file of Supplementary Material.

The Maximum Hydraulic Length (L_{Hmax}) is defined as the effective pore throat diameter corresponding to the highest hydraulic conductance. The value of L_{Hmax} is the length corresponding to the capillary pressure at which the product of the mercury saturation and the pore throat diameter, $S_{Hg} \times d_{pt}$, is maximum. Katz and Thompson introduced a permeability model based on the length scale L_{Hmax} (Katz and Thompson, 1986, 1987; Thompson et al., 1987).

$$k_{LH} = C_2 \left(\frac{L_{Hmax}^3}{L_c} \right) \phi \, S_{LHmax} \, , \qquad (2)$$

where the term L_{Hmax}^3/L_c provides the length-squared dimensions required for permeability, S_{LHmax} is the fraction of connected pore volume filled with mercury at L_{Hmax}, and the term $\phi \, S_{LHmax}$ represents the fraction of the whole rock filled with mercury at L_{Hmax}. The parameter L_c is the critical length, which is defined as the critical pore diameter at which mercury forms a connected path through the sample, as shown in Fig. 2. This occurs at the threshold pressure, which can be determined from the inflection point on a MICP curve. In this case the constant $C_2 = 1013/89$. The constant has empirical origins but is usually not varied to improve the fit or performance of the model.

2.1.2. Schwartz, Sen and Johnson [SSJ] generic form

A series of papers in the mid-80s (Johnson et al., 1986; Johnson and Schwartz, 1989; Johnson and Sen, 1988; Schwartz et al., 1989) led to the development of a characteristic length scale Λ for pores (Johnson et al., 1986), and a new permeability model which used it. A generalised form of this equation may be written as

$$k_{SSJ} = \frac{\Lambda^2}{aF}, \qquad (3)$$

where Λ is the Johnson et al. (1986) characteristic length scale of the pores, F is the formation factor and a is a constant that may be treated as a fitting parameter (Walker and Glover, 2010). This is an
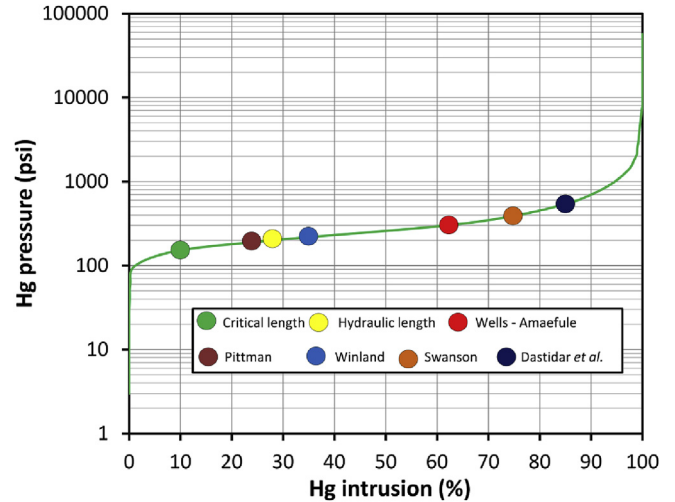
extremely simple model where the patency of the pores is expressed by the length scale and the connectedness of the pore flow paths is expressed by $1/F$.

It should be noted that the characteristic length scale of the pores is not some measure of the diameter or the radius of the pores in the usual sense; rather it is a measure of the effect of the pores on defining the transport properties of the pore network.

We cannot implement the SSJ model directly with our dataset because of the difficulty in finding an independent measurement of the characteristic length scale. Furthermore, calculation of the Λ parameter from our grain size, cementation exponent and formation factor would ensure that the SSJ model becomes formally the same as the RGPZ model. Instead, we have used Eq. (2) to generate a generic permeability model which shares some of the characteristics of both the SSJ and the RGPZ models. This equation may be written as

$$k_{GENERIC} = \frac{d_{grain}^2}{bF^3}, \qquad (4)$$

where b is an empirically-determined parameter.

Walker and Glover (2010) took four of the most important models for predicting the permeability of porous media; the classical model of Kozeny and Carman [K–C] (e.g., Bernabé, 1995), that of Sen, Schwartz and Johnson [SSJ] (Johnson et al., 1986; Johnson and Sen, 1988; Schwartz et al., 1989; Johnson and Schwartz, 1989), that of Katz and Thompson (Katz and Thompson, 1986, 1987; Thompson et al., 1987) [KT], and the RGPZ model (Glover et al., 2006a,b,c). Each of these models is derived from a different physical approach. Walker and Glover (2010) rewrote them in a generic form which implied a characteristic scale length and scaling constant for each model. After testing the four models theoretically and against experimental data from 22 bead packs and 188 rock cores from a sand-shale sequence in the U.K. sector of the North Sea, they concluded that the Kozeny-Carman model did not perform well because it takes no account of the connectedness of the pore network and should no longer be used.

They discovered that the other three models all performed well when used with their respective length scales and scaling constants. Surprisingly, they found that the SSJ and KT models produce extremely similar results and their characteristic scale lengths and scaling constants are almost identical even though they are derived

using extremely different approaches: the SSJ model by weighting the Kozeny-Carman model using the local electrical field, and the KT model by using entry radii from fluid imbibition measurements.

2.1.3. RGPZ model

Like the SSJ model, the RGPZ model (Glover et al., 2006a) is also derived analytically and does not need calibration. The original equation is derived from the theoretical result that links the characteristic length scale Λ introduced by Johnson et al. (1986) to permeability through Eq. (2) and the approximate relationship between Λ and the electrical properties of the porous medium $\Lambda \approx d_{grain}/2mF$. The result is

$$k_{RGPZ1} = \frac{d_{grain}^2 \phi^{3m}}{4am^2} = \frac{d_{grain}^2}{4am^2F^3}, \tag{5}$$

where d_{grain} is some measure of the grain size which controls the flow properties of the porous medium, m is the cementation exponent (dimensionless), and ϕ is the porosity (as a fraction). It is important to note that the constant a is usually taken as 8/3 despite it being the same parameter that appears in Eq. (2). Consequently, it may be left to vary, and if so, the equation becomes empirical. It should be noted that this constant a is not the same as the Winsauer et al. modification to Archie's law (see Glover, 2015).

It has been pointed out that Eq. (5) relies on the formation factor being much greater than unity (*i.e.*, $F >> 1$). While this is valid for clastic rocks without fractures, it may not be the case for rocks with low values of F such as those containing significant fractures. An exact form of the RGPZ equation, which is valid for all values of formation factor, can be obtained by replacing the approximation $\Lambda \approx d_{grain}/2mF$ with its exact form $\Lambda = d_{grain}/2m(F-1)$ (Revil and Cathles, 1999). This explains the failure of Eq. (5) for low F and corrects it, leading to

$$k_{RGPZ2} = \frac{d_{grain}^2}{4am^2F(F-1)^2}. \tag{6}$$

The definition of d_{grain} is critical to its implementation. For unimodal grain size distributions the use of the simple modal grain size gives permeabilities that can be overestimated. Glover et al. (2006b; 2006c) used Eq. (5) to compare the predictive powers of characteristic grain size obtained from the (i) modal value, (ii) weighted arithmetic mean, (iii) weighted harmonic mean, (iv) weighted geometric mean, and (iv) median values from grain size distributions obtained from over 42 MICP measurements on glass bead packs, sands and reservoir rocks over a range from 100 mD to 100 D. The mean values were weighted by the grain size distribution across its entire range. The weighted geometric mean provided predicted permeabilities that were closest to those measured.

While the RGPZ has no variable coefficients and is theoretical in nature, unknown parameters such as, say, the cementation exponent, might be allowed to vary whereupon the model would become empirical. This study recognises that the RGPZ model was developed for clastic rocks and relies on their being a particular relationship between the grain size and the pore and pore throat sizes that seem to hold for clastic rocks but not for carbonates. This study has developed a new empirical permeability estimation method from the RGPZ model which is described later.

2.1.4. Berg (2014) model

Recently, Berg (2014) has published a new model that attempts to use parameters that are both physically meaningful as well as being accessible experimentally. Berg's (2014) model can be written as

$$k_{BERG2014} = \frac{\tau_s^2 L_h^2 \phi_s}{8C_s}, \tag{7}$$

where τ_s is the effective hydraulic tortuosity, L_h is the characteristic length relating to the flow process and becomes equal to the radius in a capillary tube special case solution of the equation, ϕ_s is the effective porosity, and C_s is called the constriction factor, and represents how flow paths become constricted in the direction of flow just as the fluid passes from pores into pore throats and out again.

The effective hydraulic tortuosity τ_s is the same as that used in the Kozeny-Carman formulations which is represented as the shortest flow length possible (*i.e.*, the length directly across the sample of rock) divided by the flow path length. This formulation of effective hydraulic tortuosity leads to smaller values when the flow is contorted rather than direct. In petrophysics we are more comfortable with the hydraulic tortuosity becoming larger if the flow is more contorted, so we will use that definition instead, rewriting the hydraulic tortuosity $\tau_h = 1/\tau_s$. Moreover, the electrical tortuosity is considered to be equal to the square of this hydraulic tortuosity $\tau_e = \tau_h^2$ and the definition of electrical tortuosity is $\tau_e = F\phi$, which allows Eq. (7) to be recast as

$$k_{BERG2014} = \frac{\phi^{1-m}L_h^2(\phi - \phi_c)}{8C_s}, \tag{8}$$

where ϕ_c is the porosity that does not take part in fluid flow. We cannot determine ϕ_c and have therefore taken $\phi_c = 0$. We have also assumed that the characteristic length L_h can be represented by the Katz and Thompson hydraulic length L_{Hmax} used in Eq. (2). Taking all of these modifications into account the Berg (2014) model implemented in our study under the name of the 'Berg (2014) generic model' takes the form

$$k_{BERG2014} = \frac{L_{hmax}^2 \phi^{2-m}}{8C_s}, \tag{9}$$

where the constriction factor C_s is varied for the optimum fit, and hence the equation is used by use as an empirical relationship.

2.2. Poiseuille-based models

2.2.1. Winland method

The models of Swanson, Wells and Amaefule and Kamath are all, in effect the same, differing only in the dataset upon which they have been calibrated. Winland, however, introduced a new approach, where the length scale was that at which a mercury saturation of 35% is attained, or R_{35}. The value of R_{35} is simply the radius calculated using the Washburn equation (Eq. (1)) from the capillary pressure corresponding to a mercury saturation of 0.35. Winland recognised that the permeability was related to both R_{35} and the porosity ϕ with an equation of the form

$$k_{Winland} = C_4 R_{35}^{a_2} \phi^{a_3}, \tag{10}$$

where C_4, a_2 and a_3 are empirical variables, the permeability is calculated in mD and the R_{35} value is in μm.

The Winland model was originally described as a series of three unpublished reports for the Amoco Production Company, written between 1972 and 1976. These are consequently difficult to obtain and not referenced in this study. Instead we reference studies by Kolodzie (1980) and by Gunter et al. (2014), both of which discuss the Winland model in detail and the latter of which gives the full references of the original three reports.

Winland calibrated his equation using a dataset consisting of 82 samples (56 sandstones and 26 carbonates) for which he had

Klinkenberg-corrected permeabilities, and a further 240 samples for which only uncorrected air permeability data was available. The calibration gave $C_4 = 49.4$, $a_2 = 1.7$ and $a_3 = 1.47$. The range of the calibrating permeabilities is unknown but we do know, thanks to the research of Comisky et al. (2007) that they were made under ambient conditions.

The value of R_{35} is a rather crude way of defining the length scale that best characterises fluid flow in a complex medium. Nevertheless, other constant values, such as R_{40}, R_{50} have been suggested, but of those tested the R_{35} value, which corresponds to the largest pore throat sizes has been found to give the best result (Nelson, 1994; Kolodzie, 1980; Pittman, 1992).

2.2.2. Pittman model

Pittman (1992) modified the Winland equation, using the length scale that corresponds to the threshold pressure instead of R_{35}. This length scale is the same as the critical length scale used by Katz and Thompson (Katz and Thompson, 1986, 1987; Thompson et al., 1987), but is used by Pittman as a radius. The Pittman equation is

$$k_{Pittman} = C_5 R_{Apex}^{a_4} \phi^{a_5} . \tag{11}$$

Pittman calibrated this model using a set of 202 sandstone samples from 14 formations on which measured permeability, porosity, and mercury injection data had been obtained (Pittman, 1992) and obtained $C_5 = 32.3$, $a_4 = 1.185$, and $a_5 = 1.627$.

We have used our capillary pressure data to obtain a mean value for $R_{Apex} = 0.135 \pm 0.169$, corresponding to a mercury saturation of 35%. In other words, the points shown by the circles labelled Swanson and Winland in Fig. 2 are very similar, and the two models are sampling the same fraction of the pore space.

2.3. Model summary

There is a striking difference between the percolation models and those based on the Poiseuille approach. The former need few empirical constants or sometimes none at all. The latter need two or even three such constants. Consequently, it might be expected that the Poiseuille-type models would provide better fits to data which are from similar formations, due to their specificity and the advantage of having more fitting parameters. However, they will perform much worse than the percolation models if they are used to predict the permeability of rocks which do not share the characteristics of the rocks for which they were calibrated.

Most of the models used in this paper were developed for use with clastic rocks, and specifically for sandstone, with only a few being calibrated partially with carbonate samples. Even the analytical RGPZ model was developed specifically for clastic rocks and has traditionally not fared well in carbonates. The confining pressure of the measurements which were used to calibrate the samples varied as well; from between 3000 and 4000 psi for the model of Wells and Amaefule (1985) to only 800 psi or even ambient pressures in others (*e.g.*, Winland and Pittman). The permeability measurement approach also varied significantly between all the models, including air permeabilities, steady-state and unsteady state measurements, and pulse decay measurements. Some of these were corrected for slippage, while others were not. Comisky et al. (2007) provide a useful table which compares the experimental conditions of many of the permeability models listed above.

In other words, none of the methods summarised above were specifically derived for tight carbonate rock samples (*i.e.*, for permeabilities less than 1.0 mD). This study uses samples with permeabilities in the range 100 nD to 0.7 mD, and which exhibit no fractures or microcracks.

3. Materials and measurements

Two suites of samples were used in this work.

The initial assessment of all 16 of the models used a suite of 125 core plugs from the Kometan formation, originating from different outcrop locations or core material from a number of different fields in the western segment of the Zagros basin in the northern part of Iraq (Rashid et al., 2015). For capillary measurements 25 plug samples were measured, of which 3 failed to imbibe mercury because their pores were highly cemented. The effective porosity of the samples ranged from 0.02 to 0.25, with a precision of ± 0.005, while their permeability ranged from 10 nD to 500 μD.

The validation testing on the newly developed RGPZ Carbonate model, the generic model and the two original RGPZ models used a suite of 42 core plugs from the Solnhofen limestone from a quarry near Blumenburg. The samples show a range of effective porosity from 0.11 to 0.14 with a mean of 0.044, measured with a precision of ± 0.005, and which had a permeability range from 11.5 nD to 176 μD.

Prior to making any measurements, the cores were cleaned and dried using a Soxhlet extraction process with low-temperature chloroform-methanol solutions according to the American Petroleum Institute (API) recommended practices for core analysis. The samples were then dried in a humidity-controlled environment. These cleaning and drying protocols were initiated in order to reduce the effect of any damage or alteration of rock materials, especially the clays that might enlarge pore spaces (Gant and Anderson, 1988).

The effective porosity of all the Kometan samples was measured by helium porosimetry using a Quantachrome stereopycnometer in the Wolfson Laboratory at the University of Leeds, while the Solnhofen samples were measured using a high resolution helium porosimeter that was designed and built by one of the authors of this paper and resides in the Petrophysics Laboratory of the University of Leeds. The permeability of each sample was measured using a helium pulse decay Klinkenberg-corrected permeability approach. These measurements involve measuring the decay of gas pressure in an upstream reservoir as the gas leaks through the sample. The measurements were carried out using a helium gas pulse decay permeameter such as that in the Wolfson Laboratory of the University of Leeds (Jones, 1997). At least four pulse decay tests were carried out for each rock sample, each with different initial up-stream gas pressures in the range between 50 and 200 psi and downstream pressures arranged such that the initial differential pressure was in the range of 5–40 psi. All measurements of the Kometan limestone samples were made using a net confining pressure of 800 psi, while all the Solnhofen samples were made at a net confining pressure of 725 psi, and at a temperature of 25° C in each case. The net confining pressure is very important for tight rocks as permeability can vary greatly as a function of this parameter. All permeability measurements were corrected for slippage effects as these can also be very significant in tight rocks.

Considerable efforts were made to optimise the quality of these small porosity and permeability measurements, including the preparation of high quality cylindrical core plugs.

The capillary pressure curve was measured using a high pressure mercury injection capillary pressure technique, which involves injecting mercury into an evacuated core sample in a stepwise fashion (Melrose, 1990). The volume of mercury injected at each pressure is a measure of the non-wetting (*i.e.*, mercury) saturation. This method is relatively fast, usually requiring only hours to complete each measurement. In addition, MICP techniques are capable of applying injection pressures as great as 60,000 psi, which provides coverage of almost the entire range of water saturation and capillary pressure for tight carbonate rock samples, as well as for higher porosity and permeability reservoir quality rocks

(Torsaeter and Abtahi, 2000). The MICP technique has some disadvantages, which include the use of mercury as a proxy for the reservoir non-wetting phase (usually a hydrocarbon) and air used as the wetting phase, when in a reservoir it is usually water. Mercury-air capillary pressure measurements made in this way require conversion to give the value they would have in a reservoir using reservoir fluids and at reservoir pressure and temperature. This correction is carried out using contact angle and surface tension measurements on the mercury-air-rock system and on the reservoir fluid-rock system at reservoir conditions. Although the MICP technique ensures that the sample cannot be used for further tests and must be disposed of safely, the technique can be used on samples with irregular shapes, including drill cuttings (Jennings, 1987). In this study tests were carried out using a MicroMeritics 33 Porotech IV apparatus (Webb, 2001). The non-wetting phase was injected using 62 pressure steps which were distributed logarithmically. The selection of penetrometer size is derived from the combination of the sample volume and porosity (Giesche, 2006). Acceptable capillary pressure results can be achieved when at least 20% of the penetrometer stem volume is displaced into the rock sample. Tight rock samples with low porosities require larger sample volumes for any selected penetrometer size. In this work penetrometers with stem volumes between 0.392 cm^3 to 1.131 cm^3 were used. A mercury-air-rock contact angle of 140° and the mercury-air surface tension of 480 dyn/cm (0.48 N/m) (Webb, 2001) was used throughout this work.

The MICP measurements were either used directly in modelling, which was usually the case for the Poiseuille-based models, or were used to calculate a modal pore throat size which could then be used to calculate a modal pore size or a modal grain size using techniques of Glover and Déry (2010) and Glover and Walker (2009), respectively, for subsequent use in modelling with the percolation-based models.

Some of the models also require the formation factor and cementation exponent to be known. These were obtained by measuring the electrical properties of each of the samples after they have been saturated with an aqueous solution. Full saturation of such tight samples is a very difficult thing to carry out. In our case it involved a combination of evacuation and saturation under a vacuum followed by pressurisation. The formation factor is best obtained by making a number of electrical measurements while the rock is saturated with pore fluids of different salinity. However, because the rocks are so tight we chose in all cases to calculate the formation factor from the electrical resistivity measured on the rock at 1 kHz while it was saturated with a single salinity of pore fluid together with the resistivity of that pore fluid. The method for doing this is straightforward and can be found in the review by Glover (2015) together with methods for measuring the resistivity of the pore fluid itself. A simple equation links the cementation exponent to the formation factor and porosity, and hence the cementation exponent for each sample can also be calculated simply, as also set out in Glover (2015).

4. Porosity & permeability

Fig. 3 shows a poroperm cross-plot of all the measured Kometan limestone data, some of which was used in the initial modelling, as well as the Solnhofen data that was used as an independent data set for testing purposes.

Fig. 3a classifies the samples according to a petrofacies classification that is discussed in Rashid et al. (2015). In this figure Petrofacies A is a compact wackstone/packstone which has lost almost all of its primary porosity due to cementation, containing nanometre-sized intercrystalline pores, and which contains occasional microfractures and styllolites and consequently has a very low

porosity and permeability. Petrofacies B is a dissolved wackstone/packstone that contains moldic and vuggy pores, and Petrofacies C is a carbonate mudstone that has undergone dissolution and possibly some dolomitisation. Fig. 4 shows typical scanning electronmicrographs for each petrofacies.

The petrophysical behaviour of the samples is controlled by a complex pore geometry system, governed by throat size, pore size and digenetic alteration. The poroperm diagram shows each petrofacies distinctly. Petrofacies A comprises the first group and is well separated from the other two petrofacies in the bottom, left-hand corner of the poroperm diagram due to its low porosity and permeability, varying between 10 nD and 10 μD (green symbols). This type of rock has porosities in the range 0.01—0.08 and a wide range of permeabilities. The large spread of permeabilities reflects the large range of pore connectivity present within this fabric, while the positive trend shows that any small increase in porosity provides an enhancement of the connectivity of the pore network sufficient to increase the permeability of the sample. There is some overlap between Petrofacies B and C (the blue and red symbols in Fig. 3, respectively), but both show significantly larger porosities and correspondingly larger permeabilities. The relatively flat poroperm trend of Petrofacies C shows that increasing porosity (in the range 0.18—0.28) is not significantly enhancing permeability in the sample, which is in the range 0.08—4 mD. This agrees well with our observation that moulds and vugs tend to be relatively unconnected to the pore network. Petrofacies B has a well constrained porosity range, from about 0.08 to about 0.25, and an equally well constrained permeability range. Overall there is a positive poroperm trend for Petrofacies B, showing that higher porosities caused by dissolution also lead to higher permeabilities (Rashid et al., 2015).

Fig. 5 shows a plot of the capillary pressure type-curves, demonstrating the full range of the capillary pressure curves within the Kometan limestone dataset. The entry pressure and displacement pressure of each group varies. A high entry pressure was recorded for all samples, reflecting the tightness of all of the samples.

From the examination of thin section and SEM results of the representative samples, we see a trend of decreasing pore size with decreasing pore throat size implying increasing entry capillary pressure values and decreasing permeability. However, there is no similar relationship between the pore size and grain size. The moldic pores have greater diameter because they are derived from the dissolution of foraminifer chambers. Consequently, there is no relationship between the size of these large moldic pores and the modal grain size of the rock. This observation allows us to predict that the models which were developed for clastic rocks and in which there is an implicit assumption that the pore and pore throat size are related to the grain size, such as the RGPZ model, may not perform well in carbonates in general and specifically in tight carbonates.

Fig. 3b shows the poroperm diagram for the Solnhofen limestone data, exhibiting a surprisingly large range of permeabilities for the zero to 0.1 porosity range. Many of these samples show a trend which overlaps that of Kometan limestone Petrofacies A.

5. A new model for tight carbonates

During our initial testing of the models with the Kometan limestone samples it became clear that a new and better model was needed for tight carbonate rocks, and we decided to try to develop one. Subsequently, this model was also tested with the Kometan limestone dataset, and then, as will be shown later in this paper, applied to another independent dataset of Solnhofen limestone.

In developing the new model we decided to take the theoretical
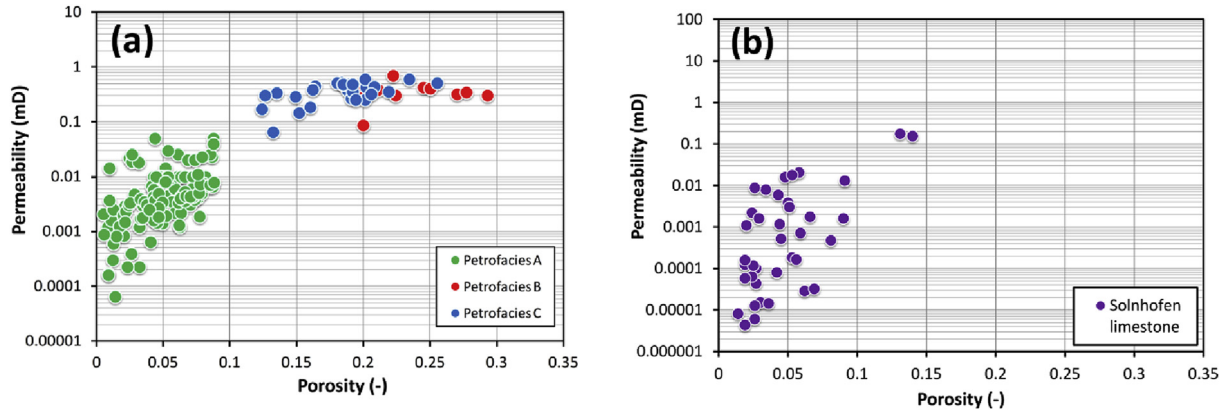
Fig. 3. (a) Poroperm cross-plot of the three facies of Kometan limestone used in this paper for initial testing of the 16 permeability models, and (b) Poroperm cross-plot of the Solnhofen limestone data that was used as an independent data set for testing four of the better-performing models including the newly developed RGPZ Carbonate model.

RGPZ model as a starting point for a number of reasons. First, one of the authors had many years understanding the model having been one of those developing it initially. Second, the model has a theoretical pedigree so that any modifications made to ensure that it performs better in carbonate rocks can be understood as simple perturbations to an already well-understood relationship, rather than a complex interaction with previous empirical developments. Third, the model had shown itself to already be fairly good at predicting the permeability of carbonate rocks, being ranked third and fourth of the sixteen models were initially tested. Finally, it was thought that the reasons behind the failure of the RGPZ model in tight carbonates was known, and might be corrected for by modification.

In clastic rocks there is a relationship between pore size and grain size. This arises from the fact that clastic rocks are composed of eroded grains which are usually sub-spherical. When the clastic rock contains some grains which have a plate-like shape, such as micas, they are usually not present in a fraction sufficiently large enough to cause gross changes to the microstructure of the pores. In this scenario, increasing the size of grains clearly increases the size of the pores, and one might think that the pore throats would increase in size as well. This idea has led to a mathematical transformation between pore size and grain size for clastic rocks to be produced (Glover and Walker, 2009), where the coefficient proportionality between the pore size and grain size is called the 'theta' transformation, and depends upon the cementation exponent m, the formation factor F, and the constant $a = 8/3$. The relationship in clastic rocks between pore size and grain size holds good providing there has not been significant diagenesis that alters the amount and distribution of pore space within the rock.

In carbonates, however, it is common that there has been a large amount diagenesis, which has altered the distribution of pore spaces within the rock by successive episodes of dissolution, precipitation and recrystallisation. In this case, there is no simple or unique relationship between grain size and pore size. Indeed, grains may be very large, complex and interlocking with each other, while the pore spaces between them have small volumes and are linked by tortuous pore throats. Increasing grain sizes are now not necessarily related to increased pore sizes, and if they are the relationship will be very different to that for clastic rocks. However, analysis of the results in this paper for the two conventional RGPZ models shows them to do fairly well, but tend to overestimate the measured permeability. We therefore hypothesise that we may get a much better prediction by scaling the theta transformation, associating increases in grain size with smaller increases and pore

size. The RGPZ model uses a modal grain size as a length scale. However, it is a pore or pore throat length scale that will ultimately control fluid flow. The implication is that we will still be able to use an RGPZ-style model, with a grain size input parameter, for carbonate rocks but the scaling factor will then take account of the fact that the input grain size is not necessarily associated with pore size as large as it would be if the rock was a clastic rock.

The use of a grain size as an input parameter ensures that the RGPZ model is easy to apply with widely available core data, but it implies that the RGPZ model incorporates a relationship that converts, or interprets the grain size in a way which can influence a predicted permeability as a pore or pore throat scale would. The question, therefore is whether this internal relationship, which has been proven to work well for clastic rocks (Glover et al., 2006a,b,c) is also applicable to carbonates.

Consequently, we have produced a new model by taking the RGPZ exact model and scaling the formation factor by an arbitrary factor η which is greater than unity, leading to a larger formation factor than would be expected from the porosity and cementation exponents of the samples. This process recognises that the connectedness of the pores involved in fluid flow is less in carbonates than in a clastic rock of the same grain size. This process converts the theoretical RGPZ model into an empirical model because the η-factor is now an empirically-determined coefficient that can be viewed as a fitting parameter. The resulting equation is

$$k_{RGPZCarbonate} = \frac{d_{grain}^2}{4am^2\eta F(\eta F - 1)^2} \approx \frac{d_{grain}^2}{4am^2\eta^3 F^3}. \quad (12)$$

The approximation is valid in the limit $F \gg 1$, and applies in this study because the formation factors in tight carbonate rocks are generally very high, varying between 23 and 2565 with a mean value of 314. The approximation will also be valid for most reservoir rocks, even those with relatively high porosities.

Since the variation of η for individual samples would result in the trivial result of a perfect prediction, we have shown the result for $\eta = 1.73$ in Fig. 6f. This value was chosen as the centre of the range in which the fitting statistics were optimised. It is worth noting that in the limit $F \gg 1$, the implementation of $\eta = 1.73$ is the equivalent of having a formation factor or tortuosity that is 73% higher, a cementation exponent 9.53% higher (for $F = 314$), or a grain, pore or pore throat size that is 43.9% of that assumed by the standard RGPZ model, accounting for the observation that diagenetic processes in carbonates have reduced the effective pore size with respect to the effective grain size.
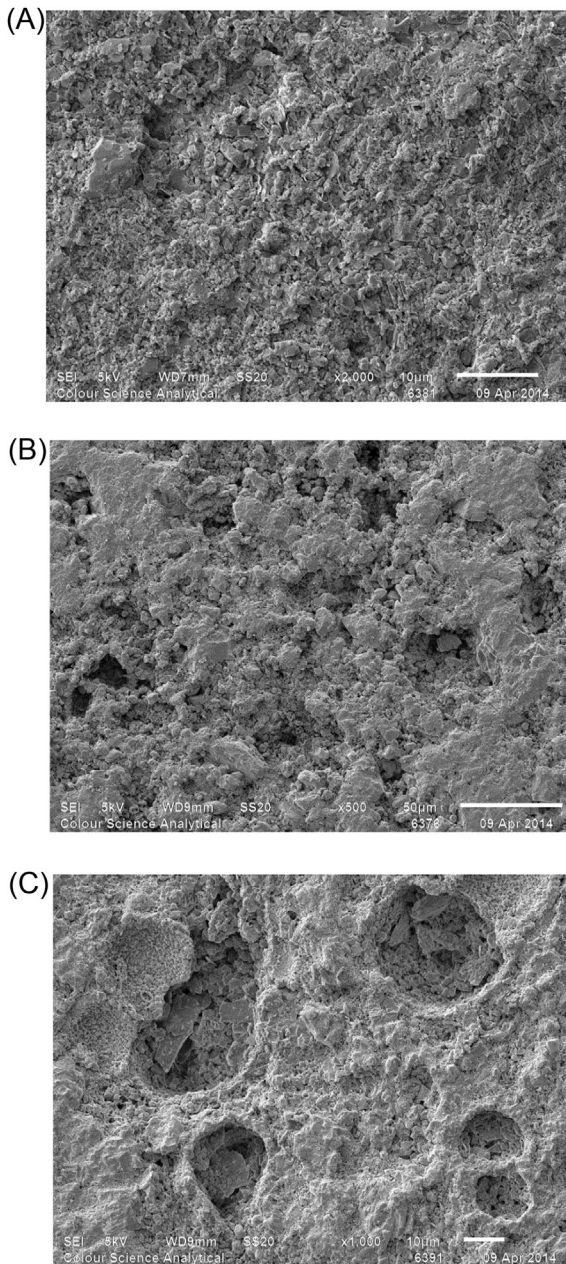
Fig. 4. Scanning electronmicrographs of the three facies of rocks studied in this work; Petrofacies A, upper; Petrofacies C, middle and Petrofacies B, lower.

Fig. 5. Mercury injection capillary pressure curves for typical samples from each of the three petrofacies used in this work.

6. Permeability prediction

In total we tested 16 models and all are included in Table 1 for completeness. This number includes the model that we have developed in this paper and describe later in the paper. Eight of the models performed particularly badly when applied to tight carbonates. Consequently, they are not reported in detail in this paper. However, their full description, concordance plots and discussion is presented in a file of Supplementary Material available from the publishers website. These models are those of the Katz-Thompson using critical lengths and electrical length (Katz and Thompson, 1986, 1987; Thompson et al., 1987), the Swanson model (Swanson, 1981), the Wells-Amaefule model (Wells and Amaefule, 1985), the Kamath model (Kamath, 1992), the Huet et al. model (Huet et al., 2005), and the Berg Fontainebleau model (Berg, 2014).

The remaining eight models, which are described further in this paper are the Katz-Thompson model using hydraulic length models (Katz and Thompson, 1986, 1987; Thompson et al., 1987), the Berg generic model (Berg, 2014), the Winland (Comisky et al., 2007; Gunter et al., 2014) and Pittman models (Pittman, 1992), the exact and approximate forms of the original RGPZ model, a generic form of the RGPZ/SSJ model (Glover et al., 2006a,b,c), and finally the model developed in this paper, which is a modification of the RGPZ model for carbonate rocks, and which we have called the RGPZ Carbonate model.

Fig. 6 shows how well each of the models predicts the measured permeability for each sample of the Kometan limestone dataset. Each part of Fig. 6 contains a 1:1 line that indicates a perfect prediction as well as high and low bounds representing a variance of ± 2.5 (i.e., upper and lower bounds representing 2.5 times greater or less than a perfect prediction, respectively). A simple judgement concerning the goodness of prediction is that the prediction falls between the variance ± 2.5 limits.

Percolation-type models tend to perform better than Poiseuille-type models, with only two of the Poiseuille-based models performing well enough to be discussed in the main paper. These are the models of Pittman and of Winland. Of the percolation models that did not perform well, two only failed marginally − the critical length and electrical length models of Katz and Thompson (Katz and Thompson, 1986, 1987; Thompson et al., 1987), while the Berg (2014) model specific to Fontainebleau sandstone, unsurprisingly failed in carbonates.

The best performance was that of the Generic model and occurred for a value of $88 < b < 100$. The new RGPZ empirical carbonate model also performed well with $1.7 < \eta < 1.76$. Both the exact and approximate forms of the standard RGPZ model (Glover et al., 2006a,b,c) also performed creditably, but produced a tendency to overestimate the permeability occasionally by as much as an order of magnitude. Since the formation factors of tight carbonate rocks are so high we might expect the two forms of the model to produce very similar results. This is borne out by Fig. 6. Calculation of the mean ratio of the permeability predicted using the approximate form of the model to that using the exact form gives 0.979 ± 0.0023, showing how close the predictions are, and that the approximate form produces slightly lower predicted permeabilities.

Of the Katz and Thompson (Katz and Thompson, 1986, 1987;
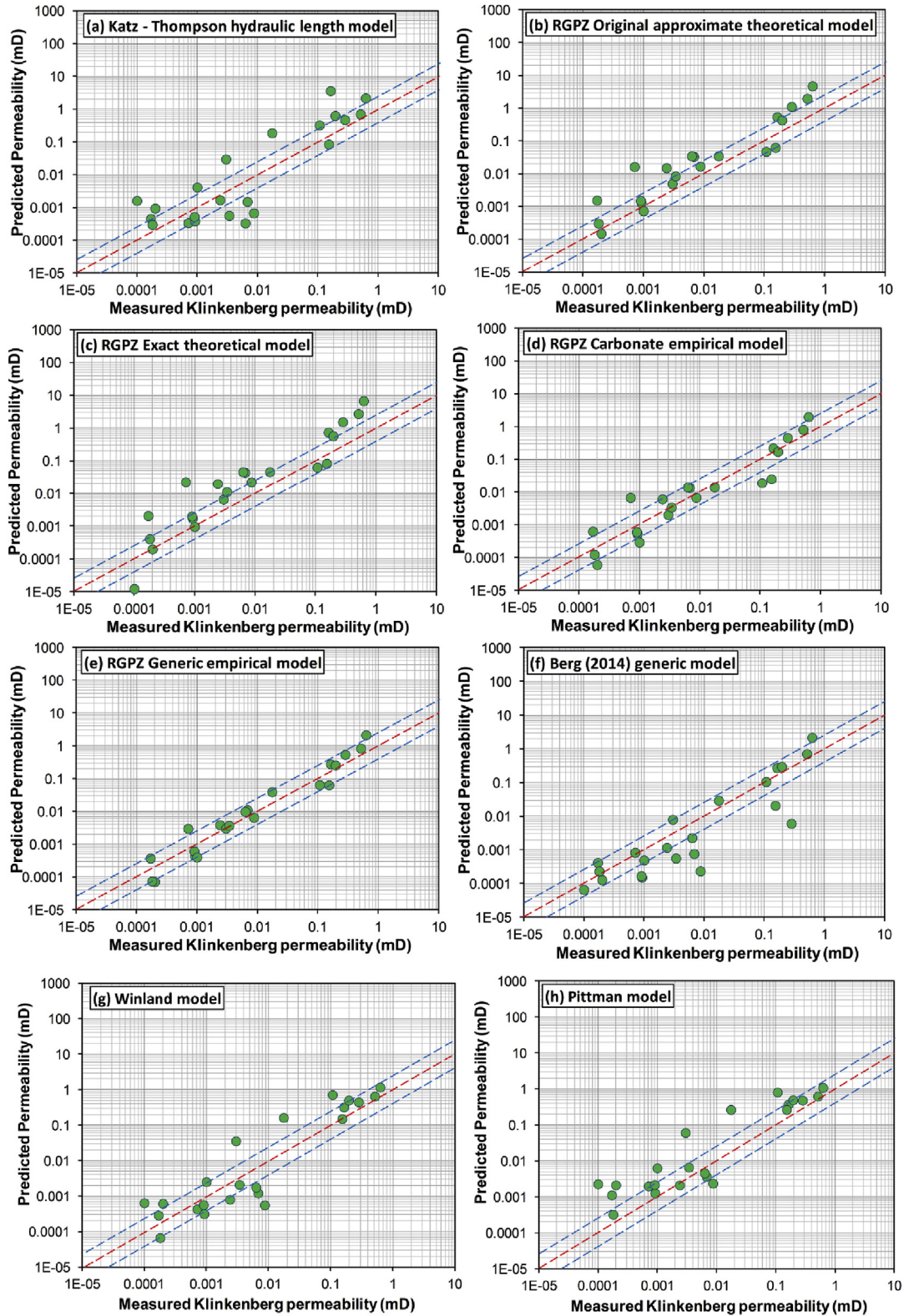
Fig. 6. The performance of the 8 best models in predicting the permeability of a suite of Kometan limestone samples, together with a 1:1 perfect agreement and variance lines set at ±2.5. For (e) $b = 94$, (d) $\eta = 1.73$, and (f) $C_s = 3.4$.

Thompson et al., 1987) models, the hydraulic conductivity model produced the best match with the measured Klinkenberg-corrected permeability for these tight carbonates. However, while the general trend of the permeability predicted with this technique matches the measured permeability well, there is a large scatter and individual samples may have permeabilities up to an order of magnitude larger or smaller than the real permeability.

The two best Poiseuille-based models were those of Pittman

(Pittman, 1992; Kolodzie, 1980; Comisky et al., 2007; Gunter et al., 2014) and of Winland (Gunter et al., 2014), with the majority of the predictions falling within the ± 2.5 variance criterion. The Winland model is one of the simplest that we have, and it is instructive that it was calibrated using Klinkenberg-corrected permeabilities. Nevertheless, the success of the Winland model for our data and possibly other tight carbonates might rely on a happy coincidence that its use of a mercury saturation of 35% upon which to base the length scale is close to the value for rocks which share the texture (porosity and connectedness) of tight carbonates.

The Pittman model (Pittman, 1992) is a modification of the Winland model using a length scale corresponding to the threshold pressure instead of R_{35}. For the rocks studied in this work the Pittman model provided predictions of permeability that were a slight improvement on those from the Winland model, over estimating permeability by about half an order of magnitude. The use of the threshold pressure instead of R_{35} led, in our study to an increase in the predicted permeability by a factor that was greater than unity in all but 3 samples and had an arithmetic mean of 2.62 ± 1.31 using standard deviation to express the uncertainty. It is clear from a comparison of these two models that, at least for the tight carbonate rocks in our data, the length scale which controls the permeability of the rock sample is closer to that associated with the threshold pressure than that associated with the R_{35} point, and is larger than the length scale associated with the R_{35} point.

We have quantified the performance of the prediction using three measures. These are: (i) the percentage of samples with predictions falling within ± 2.5 times the measured permeability, to which we give the symbol ξ, (ii) the root mean squared residual of log values (RMSLR), and (iii) the Pearson product—moment correlation coefficient (PPMCC). The RMSLR is calculated using the equation

$$RMSLR = \sqrt{\frac{1}{n} \sum_{i=1}^{n} \left[\log(K_{L,i}) - \log(K_{est,i}) \right]^2}, \qquad (13)$$

where n is the sample population size, $K_{est,i}$ is the value of the predicted permeability, and $K_{L,i}$ is the measured Klinkenberg-corrected permeability.

Table 2 shows the prediction performance statistics for all 16 models, for completeness. This table also gives a rank value for each test and an overall rank which is the rank of the unweighted sum of the three individual ranks. On this basis the best two models are the generic percolation model and the new RGPZ Carbonate model, and the worst two are the Berg (2014) Fontainebleau model which is a percolation-based model calibrated for this sandstone, and the Huet et al. model which is a Poiseuille-based model.

7. Testing the new model

Although the new RGPZ Carbonate model performed very well when predicting the permeability of the Kometan limestone samples, we felt that it was necessary to validate the new model by testing it against an independently obtained dataset. Consequently, we used a dataset of 42 samples of Solnhofen limestone, which have already been described in an earlier section of this paper. We did not restrict the permeability prediction to solely the new RGPZ Carbonate model, but also carried out prediction with the two original RGPZ models and the generic model. This was done so that the testing on the new RGPZ Carbonate model could be viewed in the context of other well-performing models. It was particularly interesting to us to see whether the modifications made to the existing RGPZ models made any significant improvements when used in predicting the permeability of tight carbonates.

Fig. 7 shows the results of the modelling. All four models performed creditably, but once again the two original RGPZ models have a tendency to overestimate the permeability in a subset of the samples. The Pearson product—moment correlation coefficient (PPMCC) was 0.801 and 0.797, respectively. Both the new RGPZ carbonate model (PPMCC = 0.799) and the generic model (PPMCC = 0.840) produced very good fits considering how small these permeabilities are.

It should be noted that Fig. 7 was produced by setting $\eta = 1.5$, and $b = 100$ for the new RGPZ carbonate model and the generic model, respectively. These values could be considered as fitting parameters, and varied to find the best fit for a particular rock type. We have not attempt to do so, but doing so might improve the fit marginally in each case. The value of these parameters depends upon how the grain size and pore throat sizes are interrelated. Consequently, there is the potential for finding a physical control behind these parameters in tight carbonates which would then allow them to be calculated independently.

8. Discussion

All of the models considered in this study use MICP measurements to provide a length scale from which a permeability can be calculated. In most cases, it is a single length scale that is defined on the assumption that the pore throat size at a given mercury saturation is special in that it represents the length scale that either controls or represents the permeability of the rock. Different definitions are used by different models. However, given the great complexity of rocks, it is unlikely that a length scale based on a single length measurement is likely to be effective in describing the permeability of a range of different rocks.

Another approach calculates a single effective length scale from a weighted (usually geometric) mean of all pore or pore throat sizes. The RGPZ method has been applied in this approach fairly effectively (Glover et al., 2006a, 2006b; 2006c), and the method is used in the method of Dastidar et al. (2007).

Whatever the method used to obtain the single, hopefully representative, value that is to be used as a length scale, the fact remains that it is a single value, and much of effectiveness of the prediction process depends upon it. In choosing a model, we are choosing which definition of the length scale we think will produce the most accurate permeability predictions.

Fourteen of the 16 models studied in this work contain coefficients that must be obtained empirically. These models need to be calibrated against a typical dataset where the permeability has been measured and is accurately known. It is important that these calibration measurements are made on the same type of materials and under the same conditions as the model will be applied. Consequently, the calibration for a tight carbonate should be carried out on tight carbonates using Klinkenberg-corrected pulse decay gas pressure measurements at a well-defined overburden pressure. These criteria were not fulfilled for any of the empirical models tested. There were few calibration datasets that contained any carbonates and there were no tight carbonates, while some calibration sets included tight clastic rocks. Some calibration sets used gas permeabilities with undefined flow pressures, while others used steady-state liquid permeabilities and a third group used unsteady-state pulse decay measurements. In some of these measurements the flow pressures were not controlled, and only a few calibration datasets had Klinkenberg-corrected their calibration data. Some measurements were made at low equivalent overburden pressures, while others used a consistent high value. In summary, the quality of the prediction depends upon the quality of the calibration, and that was often very poor.

Table 2
Quantitative measures of permeability prediction effectiveness.

ξ (%)	Rank on ξ	RMSLR	Rank on RMSLR	PPMCC	Rank on PPMCC	Overall rank	Permeability model	Type
81.818	1	0.402	1	0.923	1	1	Generic model (Eq. (4))	Percolation
68.182	2	0.576	3	0.917	4	2	RGPZ empirical carbonate model	Percolation
54.545	5=	0.609	4	0.920	2	3	RGPZ approximate theoretical model	Percolation
54.545	5=	0.618	5	0.915	5	4=	RGPZ exact theoretical model	Percolation
59.091	3=	0.654	6	0.903	6	4=	Winland model	Poiseuille
40.909	7	0.576	2	0.872	7	6	Pittman model	Poiseuille
59.091	3=	0.696	7	0.858	10	7	Berg (2014) generic model	Percolation
31.818	9	0.969	9	0.918	3	8	Katz and Thompson-Electrical length model	Percolation
36.364	8	0.724	8	0.575	14	9	Katz and Thompson-Hydraulic length model	Percolation
27.273	10	1.066	10	0.683	12	10	Katz and Thompson-Critical Length model	Percolation
4.545	13=	1.358	11	0.827	11	11	Wells and Amaefule model	Poiseuille
13.636	11=	1.605	12	0.613	13	12	Dastidar et al. model	Poiseuille
0.000	15=	1.976	13	0.866	9	13	Kamath 'model'	Poiseuille
0.000	15=	2.204	15	0.868	8	14	Swanson model	Poiseuille
13.636	11=	2.003	14	0.485	15	15	Berg (2014) Fontainebleau model	Percolation
4.545	13=	2.277	16	0.174	16	16	Huet et al. model	Poiseuille

ξ: Percentage of samples whose prediction is within a factor of ±2.5 of the real permeability.
RMSLR: Root mean squared log residuals, see Eq. (13).
PPMCC: Pearson product−moment correlation coefficient.

We associate the relative success of the Winland method with the fact that it was calibrated with a suite of cores that contained a significant number of carbonates, that the pulse decay permeability measurement was used and that all measurements were Klinkenberg-corrected. In all of these respects the Winland model approaches the conditions under which we measured our rock samples. It might be inferred, therefore, that the Winland model's use of a pore throat radius being filled when 35% of mercury saturation is attained is particularly valid for these tight carbonates. The slightly better predictions provided by the Pittman approach might suggest that the threshold pressure is an even better characteristic point upon which to base the pore throat scale length. The Katz-Thompson hydraulic length characteristic method also provides acceptable permeability predictions for our tight carbonate samples which implies that the highest hydraulic conductance of the Katz-Thompson model is
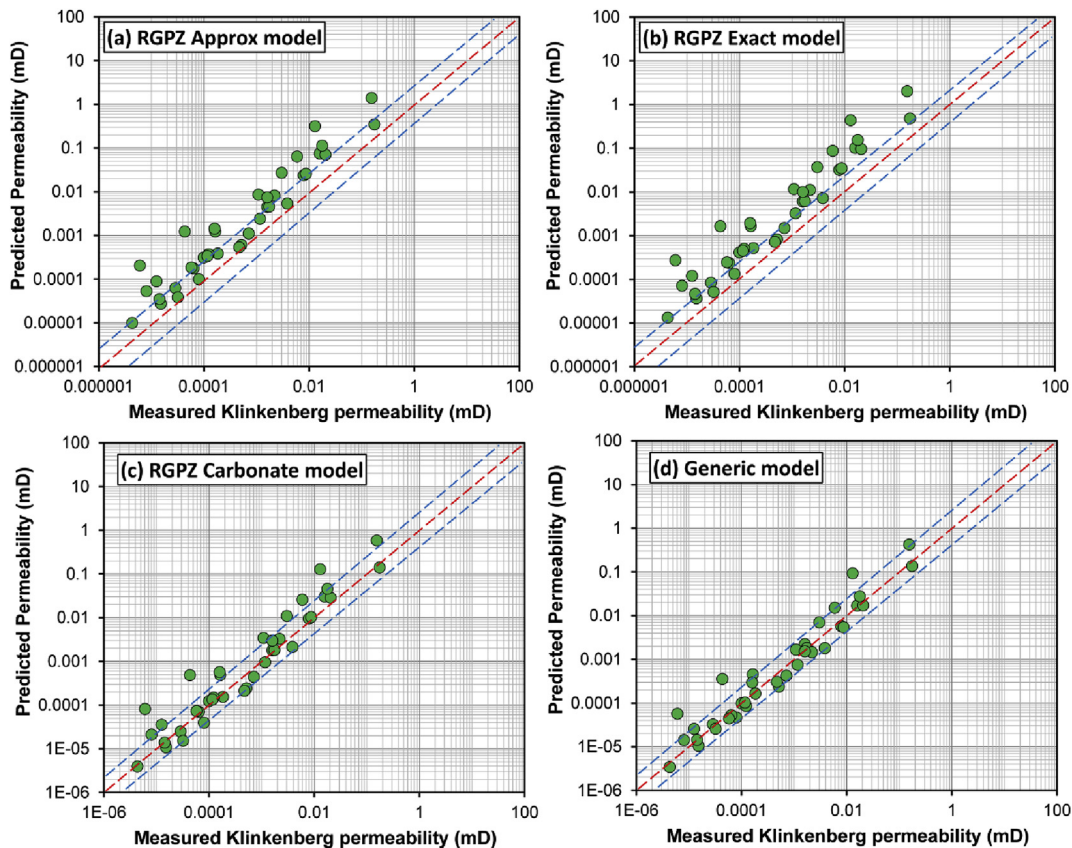
Fig. 7. The performance of (a) the RGPZ approximate model, (b) the RGPZ exact model, (c) the new RGPZ carbonate model and (d) the generic model, in predicting the permeability of a suite of 42 Solnhofen limestone samples, together with a 1:1 perfect agreement and variance lines set at ±2.5. For (c) $\eta = 1.5$, and (d) $b = 100$.

close to the R_{35} point for tight carbonate rocks. A cross-plot of the permeability predicted using the Katz and Thompson model as a function of that predicted with the Winland model shows a remarkable correlation with only a few samples not falling on a 1:1 straight line.

The Dastidar et al. (2007) model is one of the more complex models tested. It applies the weighted geometric mean approach that was used by Glover et al. (2006a; 2006b; 2006c) with the RGPZ model. The concept in using this approach is that the permeability of the rock is defined not by a single length scale, but by an ensemble of length scales from the very largest to the very smallest according to how many pores of each size compose the rock. The geometric mean is chosen because it represents the permeability of a random ensemble of sub-volumes of the sample that have individual permeabilities. Consequently, using a weighted geometric mean of the MICP pore throat sizes before applying the permeability prediction equation is equivalent to calculating the permeability with the permeability prediction equation for each pore throat size and then taking a weighted geometric mean of the resulting permeabilities, providing the permeability prediction equation is linear. All of the models investigated in this study fulfil this criterion.

Despite its complexity, the Dastidar et al. (2007) model did not perform well for tight carbonates. This may be due partly to their use of sandstones, but the previously mentioned averaging process may also be invalid in this application. It is interesting to note that the weighted geometric mean length scale (R_{wgm}) that we calculated for each sample was always significantly larger than R_{25} and R_{35}, which was the cause of the general overestimation of permeability resulting from this model. This would then imply that the weighted geometric averaging procedure was taking too much account of the largest pores in the rock. The corollary is that the largest pores in tight carbonates do not contribute much to the overall permeability of the rock, an observation that has been made previously by Rashid et al. (2015). The implication is that the weighted geometric mean approach might work in tight carbonates providing that the calculation was not done over the entire range of MICP data, but ignores the largest pores. One might also make an argument for restricting the range of the weighted geometric mean calculation to exclude the very smallest pores on the basis that these small pores would have a capillary pressure too high for the pores to transmit fluids under normal reservoir pressures.

Many of the more successful models that have been the subject of this paper use electrical data in the form of the formation factor or the cementation exponent, or both. It is interesting to ask the question whether these electrical data are accurate when made on tight rocks. It is notoriously difficult to fully saturate a tight carbonate. The formation factor measured on such a saturated tight carbonate will be that which relates to the pore network that is saturated with pore fluid. If the entire pore network is not saturated with pore fluid the measured formation factor will be higher than if it was completely saturated. It will be that higher formation factor which will be used to predict permeability, and consequently the predicted permeability will be lower than if the rock was fully saturated. The extent of this problem is difficult to gauge, and it would be a useful subject to further study. One would expect that there would be a systematic difference between the Klinkenberg-corrected permeability measured on a tight carbonate rock with a gas like helium, which can percolate through all of the pores no matter how small and the permeability measured with a liquid, and one would expect the permeability predicted using a method that require the use of the measured formation factor to also be smaller than the measured Klinkenberg-corrected gas permeability.

9. Conclusions

There are many models that purport to be able to estimate or predict the permeability of rocks for the purposes of reservoir characterisation, almost all of which were developed for high porosity and high permeability conventional clastic reservoirs. However, the current need is for models that will work in unconventional tight reservoirs which are often in carbonate lithologies, with low permeabilities, and have a degree of heterogeneity and anisotropy.

A common approach to permeability prediction uses data from mercury injection capillary pressure (MICP) measurements. We have taken sixteen MICP-based models and have tested how well they predict the permeability of a suite of tight carbonate core plugs from the Kometan formation in the north-east of Iraq. These include 7 existing percolation-based models, 8 Poiseuille-based models, and a percolation-based model that we have developed in this paper. We have included the full analysis of 8 of the models which show the best performance in this paper, and have made available the full analysis of the remaining eight in Supplementary Material which may be downloaded from the publisher's website.

All the permeability measurements presented in this paper were made by pulse decay permeametry. All measurements were Klinkenberg-corrected, and were carried out at a fixed overburden pressure of 800 psi for the Kometan limestone samples and 725 psi for the Solnhofen limestone samples. Mercury injection capillary pressure measurements were made on all samples. The permeability prediction methods often require supporting data such as formation factor, and these were made independently.

It was expected that many of the models that were developed for high permeability clastic rocks would fail badly when asked to predict the permeability of tight carbonates, and this was indeed the case. In general percolation-based models performed much better than Poiseuille-based models, though the Pittman model and Winland model performed creditably. The best performing model was the simplest, being a generic model of the percolation type upon which both the SSJ and RGPZ models are based, and both versions of the RGPZ model also performed well. Consequently, we are led to the conclusions that (i) the blind application of conventional permeability prediction techniques to carbonates, and particularly to tight carbonates, will lead to gross errors, and (ii) the development of new methods that are specific to tight carbonates is unavoidable.

There are many reasons why the predictions for many of the models are so bad. They include:

1. The models were designed for high porosity and permeability clastic rocks.
2. The models were calibrated only in the high porosity, high permeability range.
3. The models were calibrated with data that had not been Klinkenberg-corrected.
4. The models were calibrated with data made at zero or uncontrolled overburden pressures.
5. The models were calibrated using a mixture of permeability measurement approaches including methods that are irrelevant to tight rocks.
6. Carbonate rocks do not have the same relationships between grain size, pore size and pore throat size as clastic rocks due to their pore microstructure and particularly their pore connectedness being affected by post-depositional diagenesis.

Consequently, we developed a new model based on the RGPZ theoretical model by adding an empirical parameter to account for the relationship between grain size and pore throat size in

carbonates in an attempt to provide a better model for use with tight carbonates. We have tested this new RGPZ Carbonate model, together with the generic model, and the two original RGPZ models have been tested against laboratory permeability measurements made on a suite of 42 samples of tight Solnhofen carbonate. In this dataset, the permeability was measured using a Klinkenberg-corrected pulse decay technique at an overburden pressure of 725 psi. These samples were also subjected to helium porosimetry, and electrical measurements in order to obtain the formation factor and cementation exponents. Finally, each sample was submitted to Mercury Injection Capillary Pressure measurements to obtain a modal pore throat size, and modal pore sizes and grain sizes were calculated, providing a full set of measurements required to predict the permeability using the four chosen methods.

All of the four models tested at this stage performed very creditably with the new RGPZ Carbonate performing second best ($PPMCC = 0.799$). Perhaps surprisingly the best two models, the generic model and the new RGPZ Carbonate model are also simplest, containing only one empirical coefficient. It should also be remarked that the two original forms of the RGPZ model, which also performed creditably, despite being strictly valid only for clastic rocks, were the only theoretical models in the 16 tested, and consequently did not need to be calibrated with experimental data.

In the light of needing to develop new and different ways to predict the permeability of tight carbonates, it has been suggested that one approach might be to use multi-dimensional imaging techniques such as CT scanning. If this were to be successful for tight carbonates it would not only imply the use of extremely high-resolution CT scanning such as that provided by NanoXCT imagers, but also the development of software that was capable of reliably modelling fluid flow in the resulting digital pore microstructure model.

Acknowledgements

Appendix A. Supplementary data

Supplementary data related to this article can be found at http://dx.doi.org/10.1016/j.marpetgeo.2015.10.005.

References

Archie, G.E., 1942. The electrical resistivity log as an aid in determining some reservoir characteristics: Trans. Am. Inst. Mech. Eng. 146, 54—67.
Bell, J.M., Cameron, F.K., 1906. The flow of liquids through capillary spaces. J. Phys. Chem. 10, 658—674. http://dx.doi.org/10.1021/j150080a005.
Berg, C.F., 2014. Permeability description by characteristic length, tortuosity, constriction and porosity. Transp. Porous Media 103 (3), 381—400.
Bernabé, Y., 1995. The transport properties of networks of cracks and pores. J. Geophys. Res. 100 (B3), 4231—4241.
Bernabé, Y., Maineult, A., 2015. Physics of porous media: fluid flow through porous media. In: Schubert, Gerald (Ed.), Treatise on Geophysics, , second ed.vol. 11. Elsevier, Oxford, pp. 19—41.
Bliefnick, D.M., Kaldi, J.G., 1996. Pore geometry: control on reservoir properties, Walker Creek field, Columbia and Lafayette Counties, Arkansas. AAPG Bull. 80, 1027—1044.
Comisky, J.T., Newsham, K., Rushing, J.A., Blasingame, T.A., 2007. A comparative study of capillary-pressure-based empirical models for estimating absolute permeability in tight gas sands. In: SPE Annual Technical Conference and Exhibition, 11—14 November, Anaheim, California: CD-ROM, SPE 110050. Society of Petroleum Engineers.
Dastidar, R., Sondergeld, C.H., Rai, C.S., 2007. An Improved Empirical Permeability Estimator From Mercury Injection For Tight Clastic Rocks.
Dewhurst, D.N., Jones, R.J., Raven, M.D., 2002. Microstructural and petrophysical characterization of Muderong Shale: application to top seal risking. Pet. Geosci. 8, 371—383.
Gant, P.L., Anderson, W.G., 1988. Core Cleaning for Restoration of Native Wettability.
Giesche, H., 2006. Mercury porosimetry: a general (practical) overview. Part. Part. Syst. Charact. 23, 9—19.
Glover, P.W.J., 2010. A generalized Archie's law for n phases. Geophysics 75 (6), E247—E265.
Glover, P.W.J., Déry, N., 2010. Dependence of streaming potential on grain diameter and pore radius for quartz glass beads. Geophysics 75 (6). http://dx.doi.org/10.1190/1.3509465. F225—241.
Glover, P.W.J., 2015. Geophysical properties of the near surface earth: electrical properties. In: Schubert, Gerald (Ed.), Treatise on Geophysics, , second ed.vol. 11. Elsevier, Oxford, pp. 89—137. 2015.
Glover, P.W.J., Hole, M.J., Pous, J., 2000. A modified Archie's law for two conducting phases. Earth Planet. Sci. Lett. 180 (3—4), 369—383.
Glover, P.W.J., Zadjali, I.I., Frew, K.A., 2006a. Permeability prediction from MICP and NMR data using an electrokinetic approach. Geophysics 71 (4), F49—F60.
Glover, P.W.J., Zadjali, I., Frew, K., 2006b. Permeability Prediction from MICP and NMR Data using an Electro-kinetic Approach, Poster, EGU 2006. EGU06-A-01566, Vienna, pp. 2—7 April 2006.
Glover, P.W.J., Zadjali, I., Frew, K., 2006c. A New Equation for Permeability Prediction Derived from Electro-Kinetic Theory., Oral, GAC-MAC-SEG-SGA 2006. Abstract No. 758, Montréal,14—17 May 2006.
Glover, P.W.J., Walker, E., 2009. Grain-size to effective pore-size transformation derived from electro-kinetic theory. Geophysics 74, 17—29.
Gunter, G.W., Spain, D.R., Viro, E.J., Thomas, J.B., Potter, G., Williams, J., 2014. Winland Pore Throat Prediction Method - a Proper Retrospect: New Examples from Carbonates and Complex Systems. Society of Petrophysicists and Well-log Analysts SPWLA-2014-KKK, SPWLA 55th Annual Logging Symposium, 18—22 May. United Arab Emirates, Abu Dhabi.
Huet, C.C., Rushing, J.A., Newsham, K.E., Blasingame, T.A., 2005. A Modified Purcell/Burdine Model for Estimating Absolute Permeability from Mercury-injection Capillary Pressure Data. International Petroleum Technology Conference. Qatar, Doha. Nov. 21—23, Paper IPTC 10994.
Jennings, J.B., 1987. Capillary pressure techniques: application to exploration and development geology. AAPG Bull. 71, 1196—1209.
Johnson, D.L., Koplik, J., Schwartz, L.M., 1986. New pore-size parameter characterizing transport in porous media. Phys. Rev. Lett. 57 (20), 25642567. http://dx.doi.org/10.1103/PhysRevLett.57.2564.
Johnson, D.L., Schwartz, L.M., 1989. Unified Theory of Geometrical Effects in Transport Properties of Porous Media. Presented at 30th Annual Symposium, Society of Petrophysicists and Well Log Analysts paper E, 1—25.
Johnson, D.L., Sen, P.N., 1988. Dependence of the conductivity of a porous medium on electrolyte conductivity. Phys. Rev. B Condens. Matter Mater. Phys. 37 (7), 3502—3510. http://dx.doi.org/10.1103/Phys.RevB.37.3502.
Jones, S.C., 1997. A Technique for Faster Pulse-decay Permeability Measurements in Tight Rocks.
Kamath, J., 1992. Evaluation of Accuracy of Estimating Air Permeability from Mercury-injection Data.
Katz, A.J., Thompson, A.H., 1986. Quantitative prediction of permeability in porous rock. Phys. Rev. B 34, 8179—8181.
Katz, A.J., Thompson, A.H., 1987. Prediction of rock electrical conductivity from mercury injection measurements. J. Geophys. Res. Solid Earth 92, 599—607.
Kolodzie Jr., S., 1980. Analysis of Pore Throat Size and Use of the Waxman-smits Equation to Determine Ooip in Spindle Field. Society of Petroleum Engineers, Colorado.
Lucas, R., 1918. Ueber das Zeitgesetz des Kapillaren Aufstiegs von Flussigkeiten. Kolloid Z 23, 15. http://dx.doi.org/10.1007/bf01461107.
Melrose, J.C., 1990. Valid Capillary Pressure Data at Low Wetting-phase Saturations (Includes Associated Papers 21480 and 21618).
Nelson, P.H., 1994. Permeability-porosity Relationships in Sedimentary Rocks.
Pittman, E.D., 1992. Relationship of porosity and permeability to various parameters derived from mercury injection-capillary pressure curves for sandstone. AAPG Bull. 76, 191—198.
Rashid, F., Glover, P.W.J., Lorinczi, P., Collier, R., Lawrence, J., 2015. Porosity and permeability of tight carbonate reservoir rocks in the north of Iraq. J. Petroleum Sci. Eng. 133, 147—161. http://dx.doi.org/10.1016/j.petrol.2015.05.009.
Revil, A., Cathles, L.M., 1999. Permeability of shaly sands. Water Resour. Res. 35, 651—662.
Robinson, R.B., 1966. Classification of reservoir rocks by surface texture. AAPG Bull. 50, 547—559.
Schowalter, T.T., 1979. Mechanics of secondary hydrocarbon migration and entrapment. AAPG Bull. 63.
Schwartz, L.M., Sen, P.N., Johnson, D.L., 1989. Influence of rough surfaces on electrolytic conduction in porous media. Phys. Rev. B Condens. Matter Mater. Phys. 40 (4), 2450—2458. http://dx.doi.org/10.1103/PhysRevB.40.2450.
Swanson, B.F., 1981. A Simple Correlation Between Permeabilities and Mercury Capillary Pressures.
Thompson, A.H., Katz, A.J., Raschke, R.A., 1987. Estimation of Absolute Permeability from Capillary Pressure Measurements. Paper SPE 16794 presented at the 1987 SPE Annual Technical Conference and Exhibition, Dallas, TX, Sept. 27—30.

Torsaeter, O., Abtahi, M., 2000. Experimental Reservoir Engineering Laboratory Workbook. Department of Petroleum Engineering and Applied Geophysics, Norwegian University of Science and Technology, Trondheim, Norway (Lab rep).

Walker, E., Glover, P.W.J., 2010. Characteristic pore size, permeability and the electrokinetic coupling coefficient transition frequency in porous media. Geophysics 75 (6), E235–E246. http://dx.doi.org/10.1190/1.3506561.

Washburn, E.W., 1921. The dynamics of capillary flow. Phys. Rev. 17, 273–283.

Webb, P.A., 2001. An Introduction to the Physical Characterization of Materials by Mercury Intrusion Porosimetry with Emphasis on Reduction and Presentation of Experimental Data (Norcross, Georgia).

Wells, J.D., Amaefule, J.O., 1985. Capillary Pressure and Permeability Relationships in Tight Gas Sands. Society of Petroleum Engineers.